Lyman-α photodissociation of CH$_3$CFCl$_2$ (HCFC-141b): Quantum yield and translational energy of hydrogen atoms

ALMUTH LAEUTER,[1] HANS-ROBERT VOLPP,[1] JAI P MITTAL[2] and
RAJESH K VATSA[2,*]

[1]Physikalisch-Chemisches Institut der Universitaet Heidelberg, Im Neuenheimer Feld 253, D-69120
Heidelberg, Germany
[2]Chemistry Division, Bhabha Atomic Research Centre, Mumbai 400 085
e-mail: rkvatsa@barc.gov.in

Abstract.   The collision-free, room temperature gas-phase photodissociation dynamics of CH$_3$CFCl$_2$ (HCFC-141b) was studied using Lyman-α laser radiation (121·6 nm) by the laser photolysis/laser-induced fluorescence 'pump/probe' technique. Lyman-α radiation was used both to photodissociate the parent molecule and to detect the nascent H atom products via ($2p^2$P $\rightarrow$ $1s^2$S) laser-induced fluorescence. Absolute H atom quantum yield, ϕ_H = (0·39 ± 0·09) was determined by calibration method in which CH$_4$ photolysis at 121·6 nm was used as a reference source of well-defined H atom concentrations. The line shapes of the measured H atom Doppler profiles indicate a Gaussian velocity distribution suggesting the presence of indirect H atom formation pathways in the Lyman-α photodissociation of CH$_3$CFCl$_2$. The average kinetic energy of H atoms calculated from Doppler profiles was found to be $E_{T(lab)}$ = (50 ± 3) kJ/mol. The nearly statistical translational energy together with the observed Maxwell–Boltzmann velocity distribution indicates that for CH$_3$CFCl$_2$ the H atom forming dissociation process comes closer to the statistical limit.

Keywords.   CH$_3$CFCl$_2$; photodissociation; Lyman-α; laser-induced fluorescence.

1. Introduction

Phasing out of the ozone destroying chlorofluorocarbons (CFCs) and their replacement with hydrochlorofluorocarbons (HCFCs) have created concerns about the impact of HCFCs on the atmospheric chemistry. Since HCFCs have at least one C–H bond, they can be oxidized by OH-free radicals and O(^{1}D) atoms in the troposphere. Despite this property, they still have the potential to transport chlorine to the stratosphere where photochemical processes initiated by absorption of light in the UV and VUV wavelength region have an impact on the ozone depletion.[1]

The measurement of atmospheric concentrations of HCFC-141b (CH$_3$CFCl$_2$), which is used as a replacement for CFCl$_3$ and CFCl$_2$CF$_2$Cl, shows a rapid increase since 1994.[2] Although its production is stopped and based on the revised Montreal Protocol will be phased out by 2020, its release into the at-

mosphere is expected to increase in the coming few decades because of long-term uses of the products. In order to assess the environmental impact of the accumulation of the HCFCs in detail, different studies about the molecule in the atmosphere need to be performed. Besides atmospheric concentration measurements and 3D modelling calculations, laboratory photodissociation dynamics studies of HCFCs and in particular quantitative measurements of primary photochemical product yields play an important role in understanding the mechanisms involved in the decomposition of these molecules.

Photodissociation of CH$_3$CFCl$_2$ has been studied in the UV region. At 193 nm, the main photodissociation channel is found to be formation of Cl atom with quantum yield of near unity and a minor channel leading to H atom formation (ϕ_H = 0·05).[3,4] Rupture of C–Cl and C–H has been explained by mixed character for the σ^* antibonding orbital. At the shorter wavelengths, the Rydberg excitations come into play and the spectra become richer. Recently, photodissociation dynamics of CH$_3$CFCl$_2$

was studied at 205–209 nm by photofragment velocity map imaging technique[5] and it was inferred that in this wavelength range H atoms are produced by direct cleavage of C–H bond.

Though there are several studies in the UV region, only two studies on VUV photolysis of this molecule have been reported. Valence ionic states and dissociative photoionization of CH_3CFCl_2 in 11–19 eV were investigated with threshold photoelectron and photoionization mass spectrometry (PIMS).[6] Dissociation of energy selected $CH_3CFCl_2^+$ to form CH_3CFCl^+ was studied using threshold photoelectron photoion coincidence (TPEPICO) and synchrotron radiation.[7] Unfortunately, there is no report on VUV spectrum of CH_3CFCl_2. However, for CH_3CF_2Cl, the $3p\pi \rightarrow 4s$ Rydberg series starts at 73900 cm^{-1} and $3p\pi \rightarrow 4p$ series begins at 81300.[8] The CH_3CFCl_2 spectrum is also expected to have similar features with some shifts. Knowledge of VUV photochemistry of this molecule is essential for reliable calculation of photodissociation rates in the upper atmosphere.

In the VUV region of solar spectrum, the strongest emission line is Lyman-α (121·6 nm) due to neutral hydrogen.[1,9] The energy contained in the solar Lyman-α flux is as large as the total solar flux in 120 to 160 nm region.[10] Because Lyman-α occurs at a spectral window of molecular oxygen, solar radiation can penetrate down to about 60 km in the earth's atmosphere.[11] At these levels molecules can be photolysed by Lyman-α, thus significantly affecting the photochemistry in the upper atmosphere. For Sun and other stars with similar radiation environment, the most important wavelength being Lyman-α[12], photochemistry and identification of products at this wavelength are of great significance. Our previous work[13,14] has shown that as the wavelength decreases, H atom formation channel starts competing with Cl atom formation channel. In view of this, we have investigated the VUV photodissociation of CH_3CFCl_2 at Lyman-α wavelength and the results are reported here.

2. Experimental

Photodissociation studies were carried out in a flow apparatus (figure 1), which is similar to the one used in earlier studies.[13–15] Room temperature CH_3CFCl_2 (ABCR Chemicals, purity >99·7%) was pumped through the reactor without further purification. For calibration measurements, CH_4 (>99·998% Messers Griesheim) was used under similar condi-
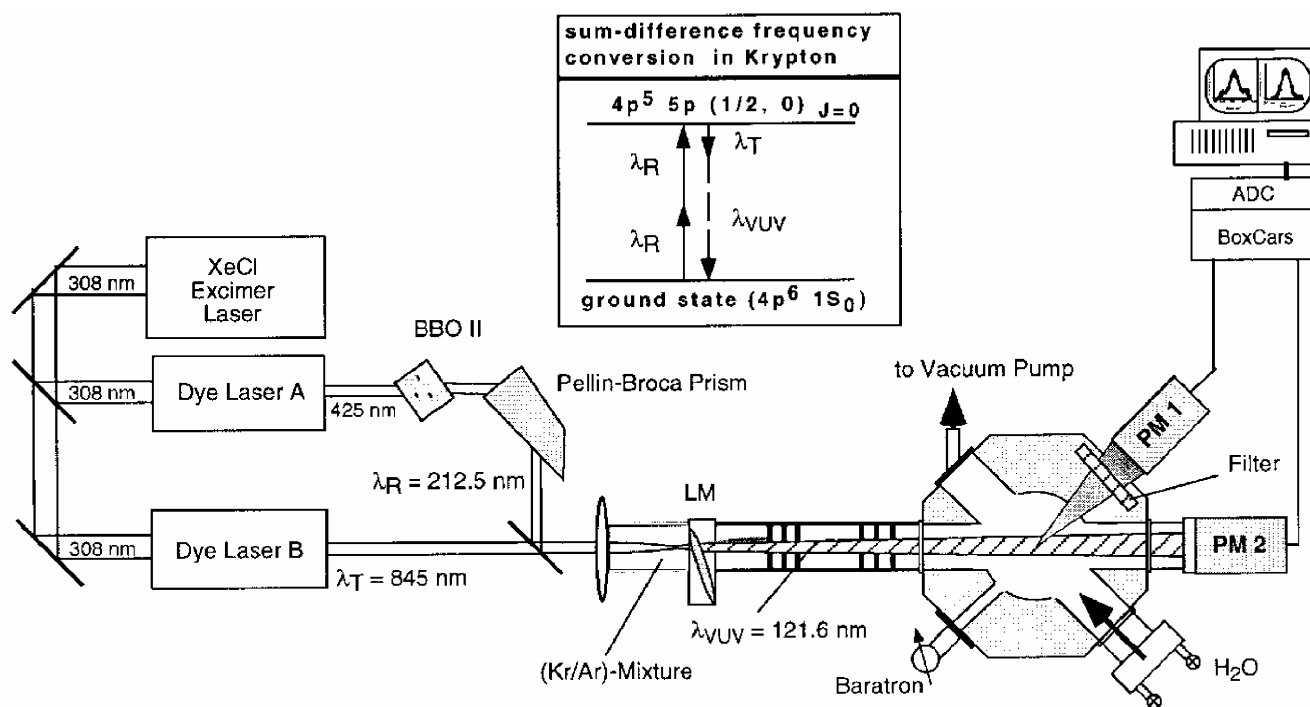

Figure 1. Experimental apparatus used for the CH_3CFCl_2 VUV photolysis studies. The Kr four-wave mixing scheme for generation of tunable Lyman-α laser radiation is shown as an inset.

tions. Typical pressures during the photodissociation experiments were 10–40 m torr as measured by an MKS Baratron.

VUV laser lights tunable around the H atom Lyman-α transition at 121·567 nm were generated by resonant third-order sum-difference frequency conversion of pulsed-dye-laser radiation in a phase-matched Kr–Ar mixture[16,17] and used to photodissociate the CH_3CFCl_2 molecule as well as to detect the photolytically produced H atom via $(2p^2P \rightarrow 1s^2S)$ laser-induced fluorescence (LIF) within the same laser pulse. The duration of the laser pulse was about 15 ns. The Kr mixing scheme via which the VUV radiation ($\alpha_{VUV} = 2\omega_R - \omega_T$) was generated is included as an inset in figure 1. The laser radiation $\omega_R = 212·55$ nm is resonant with the Kr [$4p$–$5p$ (1/2, 0)] two-photon transition and was held fixed during the experiments, while ω_T was tuned from 844 to 846 nm to generate VUV radiation covering the H atom Lyman-α transition. The fundamental laser radiation was obtained from two-dye-lasers (Lambda Physik FL 2002), simultaneously pumped by a XeCl excimer laser (Lambda Physik EMG 210 MSC). In dye laser A, Coumarin 120 was used to generate the 425·10 nm radiation which was subsequently frequency doubled in a BBO II crystal in order to obtain $\omega_R = 212·55$ nm. $\omega_T = 844$–846 nm was obtained directly by operating dye laser B with Styryl 9 dye. The generated Lyman-α light was carefully separated from the fundamental laser light by a lens

monochromator (denoted as LM in figure 1) followed by a light baffle system.

The H atom LIF signal was measured through a band-pass filter (ARC, Model 122-VN-ID, $\lambda_{center} = 122$ nm, FWHM = 20 nm) by a solar blind photomultiplier (Hamamatsu Model R1259, denoted as PM 1 in figure 1) positioned at right angles to the VUV laser beam. The VUV beam intensity was monitored after passing through the reaction cell with an additional solar blind photomultiplier of the same kind (PM 2 in figure 1). In order to obtain a satisfactory signal-to-noise (S/N) ratio, each point of the H atom Doppler profiles (figure 2) was averaged over 30 laser shots. The measurements were carried out at a laser repetition rate of 6 Hz. The LIF signals and the VUV beam intensity were recorded with a two-channel boxcar integrator system (SRS 250) and transferred to microcomputers via an analog-to-digital converter (SRS 235) where the LIF signal was normalized point-by-point to the square of the VUV laser intensity. Bearing in mind that sequential multiphoton absorption ($n > 2$) may distort the results, the $n = (1 + 1)$ photon nature (one-photon dissociation of the parent molecule followed by one-photon H atom LIF detection) of the process was checked directly in separate experiments by varying the VUV laser intensity. Log-log plots of the measured H atom LIF signal versus the VUV laser intensities yielded slopes of $n = (2·1 \pm 0·2)$ and $n = (1·9 \pm 0·1)$ in the case of CH_3CFCl_2 and CH_4 photolysis, respec-
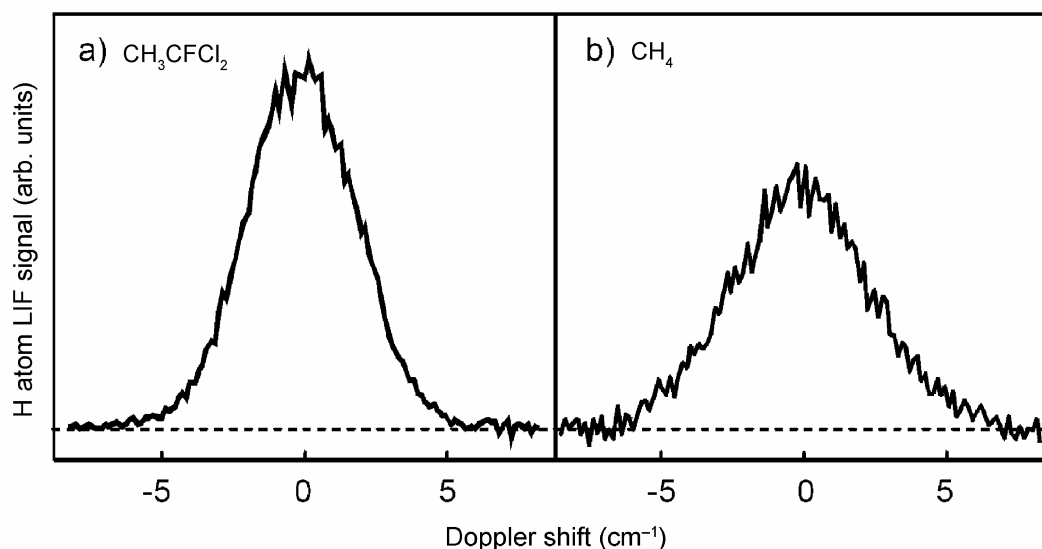
Figure 2. Doppler profiles of H atom formed on 121·6 nm photodissociation of (**a**) 9 m torr CH_3CFCl_2 and (**b**) 32 m torr CH_4. The mid-point shows the H atom Lyman-α transition at 82259 cm^{-1}.

tively. It is therefore concluded that secondary dissociation of photolysis products is negligible and need not be considered in the analysis of the results.

3. Results and discussion

3.1 *Absolute quantum yield for formation of hydrogen atoms*

The quantum yield for the formation of H atoms was measured by means of calibration against methane photolysis using the following equation[13–15]

$$\phi_H = \frac{\gamma S_{H(CH_3CFCl_2)} \phi_{H(CH_4)} \sigma_{CH_4} p_{CH_4}}{S_{H(CH_4)} \sigma_{CH_3CFCl_2} p_{CH_3CFCl_2}},$$

where σ is the absorption cross-section of molecule at 121.6 nm, S_H is the area under the H atom Doppler profile and p the pressure of the respective molecule. For the absorption cross-section values at 121.6 nm, $\sigma_{CH_4} = (2 \pm 0.2) \times 10^{-17}$ cm^2 and $\sigma_{CH_3CFCl_2} = (6.6 \times 0.5) \times 10^{-17}$ cm^2 were used.[18] The γ factor accounts for different absorption cross-sections of CH$_4$ and CH$_3$CFCl$_2$ at Lyman-α wavelength under the present experimental conditions was (0.99 ± 0.04). The quantum yield of H atom formation in methane photolysis was measured in previous work to be (0.47 ± 0.11).[19,20] Using this method, the quantum yield of H atom formation in 121.6 nm photolysis of CH$_3$CFCl$_2$ was measured to be (0.39 ± 0.09). The experimental error is the cumulative error in the measurement of pressure, cross-section and H atom quantum yield measurements of methane photodissociation at Lyman-α.

Formation of H atoms is a minor channel for the 193 nm photodissociation of CH$_3$CFCl$_2$. However, the present experimental results show that H atom quantum yield at Lyman-α is significantly higher than 193 nm (table 1). The increase in H atom quantum yield at 121.6 nm compared to 193 nm is consistent with our earlier results in other chlorofluorocarbons such as CHF$_2$Cl and CH$_3$CF$_2$Cl.[13,14] The results are

indicative of different dissociation mechanisms at these two wavelengths. First, the nature of excitation is different at these two wavelengths. Absorption of a 193 nm photon leads to excitation in the first UV band of CH$_3$CFCl$_2$ which originates from $3p\pi \rightarrow \sigma^*$ (C–Cl) transition within the valence shell ($3p\pi$ is a lone pair orbital and σ^* is an antibonding C–Cl molecular orbital). Thus, photodissociation at 193 nm preferentially leads to C–Cl bond breaking which is supported by the experimentally measured Cl atom quantum yield values which are near unity.[3] Unfortunately, the VUV spectrum of CH$_3$CFCl$_2$ is not reported at 121.6 nm. However, for very similar molecule i.e. CH$_3$CF$_2$Cl, the $3p\pi \rightarrow 4s$ Rydberg series starts at 73900 cm^{-1} and $3p\pi \rightarrow 4p$ series begins at 81300.[8] The CH$_3$CFCl$_2$ spectrum is also expected to have similar features with some shifts. Thus, excitation at 121.6 nm leads mainly to the Rydberg state which then converts into internally excited electronic ground state and subsequent dissociation occurs on the ground state potential energy surface.[13,14] In view of this, the dissociation mechanisms are different. Secondly, the absorption cross-sections at 121.6 nm $(\sigma_{121.6} = (6.6 \pm 0.5) \times 10^{-17}$ cm^2/molecule[18]$)$ is nearly two orders of magnitude higher than at 193 nm $(\sigma_{193} = 5.58 \times 10^{-19}$ cm^2/molecule[3]$)$.

Some of the possible channels which can give rise to H atom formation are shown in table 2 along with the excess energy that will be available for partitioning into different degrees of freedom. So far no investigation has been made to probe any of the above channels and in the absence of this information, it is difficult to assign from which channel the H atoms are produced.

It is worth noting that a general trend has been observed in photodissociation of the three HCFC molecules studied. In 193 nm photolysis, H atom formation is a minor channel i.e. antibonding orbital is mainly located in the C–Cl region. However, if the photolysis wavelength is changed to 121.6 nm, the H atom formation channel becomes significant as shown in table 1.

3.2 *Translational energy of H atoms*

Average translational energy of the hydrogen atoms was measured using the following equation

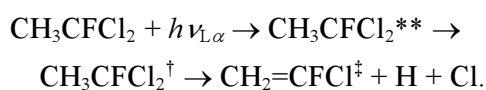$$E_H = 3 m_H \langle v_z \rangle^2 / 2 = 3 m_H (\nu - \nu_0)^2 (c/\nu_0)^2 / 2,$$

where ν is the frequency of the absorption of moving H atom as obtained from Doppler profile, c the

Table 1. Experimental results of photodissociation of CH$_3$CFCl$_2$.

Molecule	$\phi_{H\,(193\,nm)}$	$\phi_{H\,(121.6\,nm)}$	Ref
CHF$_2$Cl	(0.16 ± 0.05)	(0.77 ± 0.13)	[14]
CH$_3$CF$_2$Cl	(0.06 ± 0.02)	(0.53 ± 0.12)	[13]
CH$_3$CFCl$_2$	(0.04 ± 0.01)	(0.39 ± 0.09)	this work

Table 2. Possible reaction channels to form H atom.

Reaction channel	ΔH_R (kJ/mol)	$E_{\mathrm{avl}}^{(121\cdot6\,\mathrm{nm})}$ (kJ/mol)	
$CH_3CFCl_2 \rightarrow CH_2{=}CFCl^{\ddagger} + H + Cl$	513·1	472·1	R1
$CH_3CFCl_2 \rightarrow CHCCl + HF + Cl + H$	636·2	349·0	R2
$CH_3CFCl_2 \rightarrow CH_2CCl2 + F + H$	638·8	346·4	R3
$CH_3CFCl_2 \rightarrow CH_2CF + Cl_2 + H$	666·3	318·9	R4
$CH_3CFCl_2 \rightarrow CH_2CCl + ClF + H$	763·9	221·3	R5
$CH_3CFCl_2 \rightarrow CHCCl + F + HCl + H$	774·4	210·8	R6
$CH_3CFCl_2 \rightarrow CH_2CF + Cl + Cl + H$	908·9	76·3	R7

speed of light, ν_0 the absorption frequency of the H atom at rest and v_z the component of velocity of H atoms along the direction of the probe laser. From the measured Doppler profiles of H atoms (figure 2), the velocity of H atoms and thus the average translational energy imparted to H atoms was calculated. Doppler profiles measured in Lyman-α photolysis could be well fitted using a Gaussian fit function. The average kinetic energy of $E_{\mathrm{T(lab)}} = (50 \pm 3)$ kJ/mol was calculated from these fits. In the evaluation of H atom profiles it has to be considered that the measured line shape represents a convolution of VUV laser spectral profile and the Doppler profile of the absorbing atoms. However, the measured probe laser bandwidth of our VUV laser system is so small that a back-correction due to the finite probe laser bandwidth was well below the experimental uncertainty.

Based on only energetic considerations, it is difficult to state which of these channels is the main contributor to showing H atoms. Three-body dissociation channels R1 and R3 appear to be more probable. The H atom Doppler profiles as observed in the present study after excitation of CH3CFCl2 at the Lyman-α wavelength are similar to the ones observed in the Lyman-α photolysis of CH_3CF_2Cl,[13] CH_2Cl_2 and $CHCl_3$[14] where H atom formation has been suggested to proceed via a Herzberg I predissociation mechanism.[21] This dissociation mechanism is of an indirect type in which an internally highly excited reaction intermediate (indicated by †) can be formed by a non-adiabatic transition (via internal conversion and/or intersystem crossing) from the initially excited Rydberg state (**) to a dissociative state

$$CH_3CFCl_2 + h\nu_{\mathrm{L}\alpha} \rightarrow CH_3CFCl_2^{**} \rightarrow$$
$$CH_3CFCl_2^{\dagger} \rightarrow CH_2{=}CFCl^{\ddagger} + H + Cl.$$

Here we consider an excited molecule $CH_3CFCl_2^{**}$ dissociating into three fragments. The molecule has an energy E^* which is above the minimum energy to form the products. If there is sufficient interaction among the fragments, the distribution of fragment kinetic and internal energy can be described by statistical theory.[22] In such a case, product state distributions is characterized by a 'temperature' uniform for all product degrees of freedom.[23,24] Using the 'canonical' statistical model of Baer *et al*[25] which assumes equipartitioning of the available energy among the product degrees of freedom and treating the final fragmentation step of reaction given above as a simultaneous three-body process – a statistical 'prior' value of 47 kJ/mol is obtained for the H atom translational energy. The latter value agrees with the lower limit of the experimental value of $E_t = (50 \pm 3)$ kJ/mol. This together with the observed Maxwell–Boltzmann velocity distribution might be taken as an indication that for CH_3CFCl_2 the H atom forming dissociation process comes closer to the statistical limit. However, for a detailed understanding of UV and VUV photochemistry of CH_3CFCl_2, more information about the electronically excited states involved in the fragmentation processes is clearly needed. Further experimental studies which involve quantitative detection of other photofragments are needed before a final conclusion regarding the VUV photodissociation dynamics and related environmental impact of CH_3CFCl_2 can be drawn. Detection of other products such as F atoms, HF, HCl, $CH_2{=}CCl_2$, etc. will clarify whether the other channels are operative or not. For this purpose, mass selected time of flight investigations using a molecular beam apparatus with a universal detector based on the VUV photoionisation by synchrotron radiation will be useful.

4. Conclusion

In summary, the photolysis of CH_3CFCl_2 has been investigated at Lyman-α wavelength (121·6 nm) in

the present work. The quantum yield (ϕ_H) and average translational energy of H atoms formed during photodissociation have been measured using the vacuum ultraviolet laser-induced fluorescence. The H atom translational energy measurements suggest that a three-body photodissociation process could be operative at this wavelength. However, more work is needed to identify other products of photodissociation process. This result can contribute to the degradation process of CH_3CFCl_2 in the stratosphere and describe the model calculations.

Acknowledgement

References

1. Wayne R P 1991 *The chemistry of atmospheres* (Oxford: Oxford University Press) 2nd ed.
2. Shirai T and Makide Y 1998 *Chem. Lett.* **4** 357
3. Lauter A, Suresh D and Volpp H-R 2003 *J. Chem. Phys.* **118** 5821
4. Melchior A, Bar I and Rosenwaks S 1997 *J. Chem. Phys.* **107** 8476
5. Mashino M, Yamada H, Sugita A and Kawasaki M 2005 *J. Photochem. Photobiol. A: Chemistry* **176** 78
6. Chiang S-Y, Wang T-T, Yu J-S K and Yu C-H 2000 *Chem. Phys. Lett.* **329** 185
7. Chiang S-Y, Lee Y-C and Lee Y-P 2001 *J. Phys. Chem.* **A105** 1226
8. Doucet J, Sauvageau P and Sandorfy C 1975 *J. Chem. Phys.* **62** 355
9. Levine J S 1985 *The photochemistry of atmospheres* (New York: Academic Press)
10. Detwiler C R, Garrett D L, Purcell J D and Tousey R 1961 *Ann. Geophys.* **17** 263
11. London J 1977 *Radiation in the atmosphere* (ed.) H-J Bolle (Princeton: Science Press)
12. Jackson W M, Price II R J, Xu D D, Wrobel D, Ahmed M, Peterka D S and Suits A G 1998 *J. Chem. Phys.* **109** 4703
13. Brownsword R A, Hillenkamp M, Laurent T, Volpp H-R, Wolfrum J, Vatsa R K and Yoo H-S 1997 *J. Chem. Phys.* **107** 779
14. Brownsword R A, Hillenkamp M, Laurent T, Vatsa R K, Volpp H-R and Wolfrum J 1997 *J. Phys. Chem. A* **101** 995
15. Brownsword R A, Hillenkamp M, Laurent T, Vatsa R K, Volpp H-R and Wolfrum J 1997 *J. Chem. Phys.* **106** 1359
16. Hilber G, Lago A and Wallenstein R 1987 *J. Opt. Soc. Am.* **B4** 1753
17. Marangos J P, Shen N, Ma H, Hutchison H R and Connerade J P 1990 *J. Opt. Soc. Am.* **B7** 1254
18. Vatsa R K and Volpp H-R 2001 *Chem. Phys. Lett.* **340** 289
19. Brownsword R A, Hillenkamp M, Laurent T, Vatsa R K, Volpp H-R and Wolfrum J 1997 *Chem. Phys. Lett.* **266** 259
20. Wang J-H, Liu K P, Min Z, Su H, Bersohn R, Preses J and Larese J Z 2000, *J. Chem. Phys.* **113** 4146
21. Herzberg G 1966 *Molecular spectra and molecular structure* (Toronto: Van Nostrand) vol. III
22. Shapiro M and Bersohn R 1982 *Annu. Rev. Phys. Chem.* **33** 409
23. Freund S M, Fisk G A, Hershbach D R and Klemperer W 1971 *J. Chem. Phys.* **54** 2510
24. Kinsey J L 1971 *J. Chem. Phys.* **54** 1206
25. Baer T, DePristo A E and Hermans J J 1982 *J. Chem. Phys.* **76** 5917